ARTICLE

BIOTECHNOLOGY and BIOENGINEERING

Photopatterning of Hydrogel Scaffolds Coupled to Filter Materials Using Stereolithography for Perfused 3D Culture of Hepatocytes

Jaclyn A. Shepard Neiman,[1] Ritu Raman,[2,3] Vincent Chan,[4] Mary G. Rhoads,[1] Micha Sam B. Raredon,[1,5] Jeremy J. Velazquez,[1] Rachel L. Dyer,[1] Rashid Bashir,[3,6,7] Paula T. Hammond,[8] Linda G. Griffith[1,9]

[1]Department of Biological Engineering, Massachusetts Institute of Technology, Cambridge, MA 02139

[2]Department of Mechanical Science and Engineering, University of Illinois at Urbana-Champaign, Urbana, IL 61801

[3]2000 Micro and Nanotechnology Laboratory, University of Illinois at Urbana-Champaign, Urbana, IL 61801

[4]Department of Mechanical Engineering, Massachusetts Institute of Technology, Cambridge, MA 02139

[5]Department of Materials Science and Engineering, Massachusetts Institute of Technology, Cambridge, MA 02139

[6]Department of Bioengineering, University of Illinois at Urbana-Champaign, Urbana, IL 61801

[7]Department of Electrical and Computer Engineering, University of Illinois at Urbana-Champaign, Urbana, IL 61801

[8]Department of Chemical Engineering, Massachusetts Institute of Technology, Cambridge, MA 02139

[9]Center for Gynepathology Research, Massachusetts Institute of Technology, Cambridge, MA 02139; telephone: 617-253-0013; fax: 617-253-240; e-mail: griff@mit.edu

ABSTRACT: In vitro models that recapitulate the liver's structural and functional complexity could prolong hepatocellular viability and function to improve platforms for drug toxicity studies and understanding liver pathophysiology. Here, stereolithography (SLA) was employed to fabricate hydrogel scaffolds with open channels designed for post-seeding and perfused culture of primary hepatocytes that form 3D structures in a bioreactor. Photopolymerizable polyethylene glycol-based hydrogels were fabricated coupled to chemically activated, commercially available filters (polycarbonate and polyvinylidene fluoride) using a chemistry that permitted cell viability, and was robust enough to withstand perfused culture of up to 1 μL/s for at least 7 days. SLA energy dose, photoinitiator concentrations, and pretreatment conditions were screened to determine conditions that maximized cell viability and hydrogel bonding to the filter. Multiple open channel geometries were readily achieved, and included ellipses and rectangles. Rectangular open channels employed for subsequent studies had final dimensions on the order of 350 μm by 850 μm. Cell seeding densities and flow rates that promoted cell viability were determined. Perfused culture of primary hepatocytes in hydrogel scaffolds in the presence of soluble epidermal growth factor (EGF) prolonged the maintenance of albumin production throughout the 7-day culture relative to 2D controls. This technique of bonding hydrogel scaffolds can be employed to fabricate soft scaffolds for a number of bioreactor configurations and applications.

Biotechnol. Bioeng. 2014;9999: 1–11.

KEYWORDS: (3-6): hydrogel; stereolithography; hepatocyte; liver; patterning

Conflicts of interest: none.
Correspondence to: L. G. Griffith
Contract grant sponsor: NIH NCATS
Contract grant number: 5UH2TR000496-02
Contract grant sponsor: National Science Foundation (NSF STC Emergent Behavior of Integrated Cellular Systems)
Received 10 September 2014; Accepted 5 November 2014
Accepted manuscript online xx Month 2014;
Article first published online in Wiley Online Library (wileyonlinelibrary.com).
DOI 10.1002/bit.25494

Introduction

The liver hosts an array of homeostatic functions in the body including metabolism of nutrients, drugs and endogenous hormones, synthesis of plasma proteins, and production of bile.

In vitro physiological models of liver involving cultures of hepatocytes or co-cultures of hepatocytes with non-parenchymal cells are becoming increasingly important in assessing metabolism and toxicity of drugs and in modeling pathophysiological states of liver to understand disease processes [Griffith et al., 2014; LeCluyse et al., 2012. In the liver, hepatocytes together with non-parenchymal cells organize three-dimensionally into hexagonally shaped lobules ($\sim$1 mm) perfused through a rich sinusoidal vascular network supplied by blood from the hepatic artery and the portal vein [Godoy et al., 2013]. Most hepatocellular functions such as albumin secretion and drug metabolism decline rapidly when hepatocytes are isolated from liver and maintained in standard monolayer culture, but static culture formats that drive 3D hepatocyte aggregation into spheroids or polarization within extracellular matrix (ECM) gels can prolong maintenance of these functions in vitro (reviewed in: [Ananthanarayanan et al., 2011; Godoy et al., 2013; LeCluyse et al., 2012]). However, because hepatocytes are highly metabolically active – typically residing in close contact with blood through the fenestrated endothelium – controlling mass transfer of nutrients, substrates, and metabolites in 3D aggregates in static culture is challenging [Powers et al., 2002a]. The need for better control of mass transfer and microenvironment, together with a growing interest in incorporating non-parenchymal cells into 3D cultures as a means to better model complex liver pathophysiological processes including tumor metastasis, has driven development of a variety of perfusion bioreactor formats for 3D liver culture (reviewed in: [Ebrahimkhani et al., 2014]). These reactor systems generally strike a balance between complexity and ease of use, and particularly for polydimethylsiloxane (PDMS)-based microfluidic devices, materials of construction in the flow circuits or housing may limit applications due to partitioning of compounds into reactor components [Ebrahimkhani et al., 2014].

We have previously described a multiwell plate microreactor format in which cells are seeded directly onto a scaffold that drives 3D tissue morphogenesis via a balance of cell-cell and cell-substrate adhesion forces, and that maintains the resulting structures under continuous controlled microperfusion such that near-physiological oxygen gradients are maintained across the tissue-like structures [Dash et al., 2009; Domansky et al., 2010; Powers et al., 2002a]. The scaffold in this system comprises a thin ($\sim$0.2 mm) solid material with an array of 100–1000 through holes or "channels", each $\sim$0.3 mm $\times$ $\sim$0.3 mm, coated with collagen or other ECM. In operation, the scaffold sits upon a microporous filter that offers a high resistance to fluid flow. Thus the filter serves both to capture cells seeded into the device initially, retaining them in the channels until the cells adhere to the channel walls, and also serves as a means to distribute flow relatively uniformly through all channels in the array [Powers et al., 2002a; Powers et al., 2002b]. In these previous studies, we used scaffolds fabricated from silicon or rigid plastics. Although the proper balance of cell-cell and cell-substrate adhesion forces can drive 3D morphogenesis of liver cells even on rigid surfaces [Hansen et al., 1994; Powers et al., 1997], substrate mechanical properties and permeability to nutrients can influence hepatocellular function in culture [Coger et al., 1997; Fassett et al., 2006; Hansen et al., 2005; Moghe et al., 1996; Semler et al., 2000].

Synthetic or semi-synthetic hydrogels are attractive biomaterials for hepatocyte culture because their mechanical properties are similar to soft tissue, they have a high water content environment that facilitates the diffusion of oxygen, nutrients and removal of waste, and their synthetic counterparts can be readily tailored both biochemically and structurally to include bioadhesion ligands, growth factors, and degradation sites (Khetan et al., 2011; Lutolf et al., 2005; Underhill et al., 2007]. For example, polyacrylamide hydrogels have been employed to demonstrate that increasing mechanical compliance promotes hepatocyte compaction and liver-specific albumin secretion [Semler et al., 2005]. PEG-fibrinogen hydrogels have been structurally micropatterned using soft molding techniques to culture hepatocytes in three-dimensional micro-environments that likely facilitate the accumulation of autocrine factors to maintain high levels of liver-specific functions over a 10-day culture period [Williams et al., 2011].

Fabrication of hydrogel-based scaffolds for post-seeding in bioreactor applications generally requires three-dimensional patterning techniques to spatially control hydrogel crosslinking and the resulting scaffold's architecture. Stereolithography (SLA) is a maskless, rapid prototyping technique employed to three-dimensionally and spatially control the photopolymerization of prepolymer in a layer-by-layer fashion based on the inputted computer-aided design (CAD) file. A wide range of photocurable materials have been used to fabricate tissue engineering scaffolds with SLA to create feature sizes typically in the range of 25 to 100 μm [Melchels et al., 2010]. Among these, PEG-based materials are most commonly employed for SLA approaches, both to create scaffolds for post-seeding as well as to encapsulate cells, but most applications described thus far involve static culture systems [Arcaute et al., 2006; Bajaj et al., 2013; Chan et al., 2010; Dhariwala et al., 2004; Zorlutuna et al., 2011].

In this report, we have developed an SLA-based process to fabricate composite structures comprising PEG-based hydrogel scaffolds covalently coupled to microporous membrane filters, with the aim of developing structures that are robust to microperfusion flow and foster formation of 3D liver aggregates within the open channels of the hydrogel scaffold, adherent to the walls of the channel as described in previous reports employing stiff scaffolds [Powers et al., 2002a]. Because PEG hydrogels tend to swell post-fabrication, and swelling creates a concentrated mechanical stress at the interface between the membrane filter and the scaffold, we therefore investigated the roles of membrane composition and structure by comparing two common membrane filter types – polycarbonate (PC) and polyvinylidene fluoride (PVDF) membrane filters. We carried out a systematic investigation of parameters that influence gel delamination under the chemical and mechanical stresses of sterilization, shipping, and perfusion flow, with additional constraints of maintaining cell viability in perfused culture lasting at least 7 days. Further, we investigated the effects of cell seeding density, the magnitude of perfusion flow rate, and the addition of soluble epidermal growth factor (EGF) to the culture media on cell retention, tissue morphogenesis, and function as assessed by secretion of albumin. To the best of our knowledge, this is the first report demonstrating spatially patterned hydrogel scaffolds coupled to a filter for perfused culture of primary hepatocytes.

Methods

Filter Chemical Activation and Hydrogel Photopatterning

Track-etched, PC filters with 5-micron pore size or interwoven, PVDF filters with 5-micron pore size (Millipore, Billerica, MA) were treated with air plasma for 10 minutes using a Harrick Plasma Cleaner. Filters were subsequently soaked for 1 h in a 20% solution of ethylene diamine (Aldrich, St. Louis, MO) in PBS, pH adjusted to 10.0 +/− 0.05 with hydrochloric acid. Activated filters were rinsed for 10 mins in 1mM hydrochloric acid followed by two 10-min rinses in Millipore water. Filters were then allowed to dry at room temperature and shipped dry at ambient conditions to the University of Illinois at Urbana-Champaign (UIUC) for completion of filter activation and hydrogel fabrication.

Following arrival at UIUC, a solution of 12 mM acrylic acid N-hydroxysuccinimide ester (NHS-acryl, Sigma) solution was prepared by first dissolving 200 mg of NHS-acryl in 4 mL dimethyl sulfoxide (DMSO, Fisher Scientific, Pittsburgh, PA), and then dissolving this solution in 96 mL of 1X phosphate buffered saline (PBS, Lonza, Allendale, NJ). Aminated filters were immersed in this solution in the dark for 3 h. After soaking, filters were dried in the dark for 3 h, and then taped to glass coverslips with the treated side facing up. The glass coverslips and filters were then taped to a 35 mm dish that had been rendered hydrophilic via oxygen plasma treatment.

The pre-treatment solution for the filters consisted of 20% (v/v) poly(ethylene glycol) diacrylate of M_W 700 g mol^{-1} (PEGDA 700, Sigma-Aldrich) dissolved in PBS, with 2.5% (w/v) 1-[4-(2-hydroxyethoxy) phenyl]-2-hydroxy-2-methyl-1-propanone-1-one photoinitiator (Irgacure 2959 or I2959, BASF, Chicago, IL) mixed from a 50% (w/v) stock solution in dimethyl sulfoxide (DMSO, Fisher Scientific). 500 μL of this pre-treatment solution was pipetted onto each prepared filter. The filters were incubated in this pre-treatment solution in the dark for 2 mins, followed by gentle aspiration of the pre-treatment solution from the filter surface.

A polymerization solution of 20% (v/v) PEGDA 700 containing 0.5% (w/v) Irgacure 2959 was prepared and 900 μL of this solution was pipetted onto each prepared filter immediately after photoinitiator pre-treatment to form a liquid macromer layer 0.105 mm. Hydrogel scaffold designs were generated in the form of CAD files using SolidWorks CAD Software (Dassault Systemes, Velizy, France) and exported to stereolithography (STL) format. These files were then prepared in 3D Lightyear Software (3D Systems, Rock Hill, SC) to slice the files into 2D layers of a specified thickness. In this case, hydrogel scaffolds were polymerized onto the filters using a single-layer process at an energy density of 513 mJ/cm^2, unless noted otherwise, using a stereolithography apparatus (SLA, 250/50 3D Systems, Rock Hill, SC). The SLA operates a 325 nm ultraviolet laser with a nominal laser beam width of 250 μm. Since the effective beam width illuminating hydrogel precursor solution during crosslinking corresponds to the limiting feature size, the beam width is equivalent to the resolution of the SLA for non-swelling materials.

We have previously reported the threshold energy density, E_c, required to crosslink solutions containing 20% PEGDA-700 and 0.5% (w/v) I2959 as 41 mJ/cm^2 and measured a molar extinction coefficient for I2959 at the illumination wavelength (325 nm) as 677 M^{-1}cm^{-1} [Chan et al., 2010; Chan et al., 2012] leading to a molar extinction coefficient for these conditions of 15 cm^{-1}. Hence, for a nominal macromer solution depth of 105 m above the filter, a minimum illumination energy density of 48 mJ/cm^2 would be required to achieve crosslinking at the filter-macromer interface. However, energy intensities the energy attenuation properties of the filters are unknown, and thus we investigated intensities 3x and 11x this minimum threshold to find conditions that adequately crosslinked the precursor throughout the filter region. Unless otherwise noted, scaffolds were polymerized at an energy density of 513 mJ/cm^2.

The average energy density is a function of the laser power and laser scan speed. The SLA laser power is constant, thus energy density is modulated by adjusting the laser scan speed. To polymerize the photosensitive resin into the hydrogel scaffold design, the laser first traced the outer border of each scaffold. The laser was then rasterized across the surface of the resin in a process termed "hatching". The hatch process was performed in two steps: 1) horizontal parallel traces with a user-defined hatch spacing; 2) vertical parallel traces with a user-defined hatch spacing. In this case, hatch spacing was specified as 125 μm, corresponding to half the nominal laser beam width, to ensure planar and homogeneous polymerization of the layer pattern. Following the hatching process, the laser traced the borders of individual open channels in order to precisely define features in the polymerized part. Therefore, while hatch areas were illuminated two times by overlapping horizontal and vertical traces, the areas where border and hatch traces overlap (surrounding each channel) were illuminated three times. This resulted in a greater density of crosslinking in these border regions of the open channels, as can be observed by the increased opacity of the hydrogel (Figure 1C). Fabricated parts were rinsed, stored, and shipped to Massachusetts Institute of Technology (MIT, Cambridge, MA) in PBS in coplin jars. Upon arrival at MIT, hydrogel scaffolds were transferred to 12 well plates with 2 mL of 70% ethanol per well for sterilization and removal of unreacted constituents. After 2 h, the 70% ethanol solution was aspirated and replaced with 2 mL of sterile PBS per well and stored at 4 °C. Scaffolds were imaged with phase microscopy and final channel dimensions were measured in ImageJ (NIH).

Hepatocyte Isolation, Seeding, and Maintenance

Primary cells were perfused from male Fisher rats weighing between 180–220 g as previously described using 10 mg/L Liberase TM Research Grade (Roche, Indianapolis, IN) instead of Blendyzme III [Mehta et al., 2010]. Following the perfusion, cell suspensions were centrifuged at 50 g at 4 °C for 3 mins. The supernatant was removed and the cell pellet was resuspended in Dulbecco's Modified Eagle's Medium (DMEM) supplemented with 2 g/L BSA and 50 mg/L gentamycin (DAG). The centrifugation process was repeated and the hepatocyte-rich fraction was resuspended in DAG for a second time. Cell viability and concentration was measured on a ViCell counter.

Sterilized hydrogel scaffolds were soaked in 1:100 solution of rat tail collagen I (BD Biosciences, Bedford, MA) in 1xPBS, pH 7.4 for 1 h at room temperature. For 2D controls, tissue culture treated 24 well plates were coated with 0.5 mL of 1:100 collagen I solution. After incubation, coated wells were washed once with 0.5 mL 1x PBS.

Hepatocyte cell solutions of 1×10^6 cells/mL were prepared with seeding medium:

DMEM supplement with 0.03 g/L L-proline, 0.10 g/L L-ornithine, 0.305 g/L niacinamide, 2 g/L BSA, 2.25 g/L D(+) glucose, 2 g/L D(+) galactose, 54.4 μg/L ZnCl2, 75 μg/L $ZnSO_4$ $7H_2O$, 20 μg/L $CuSO_4$ $5H_2O$, 25 μg/L $MnSO_4$, 50 mg/L gentamycin, 10 mM HEPES, 0.1 μM dexamethasone, 1 mM L-glutamine, 10 mg/L insulin transferrin sodium selenite containing 10% FBS, and 0.3 mL cell solution was pipetted into the bioreactor or onto collagen coated plates (2 cm^2/well) at a density of 75,000 cells/cm^2 for 2D controls. Soluble EGF was supplemented to media where indicated at a final concentration of 20 ng/mL.

Cells seeded on top of scaffolds within the bioreactor were initially cultured under 1 μL/s downward flow in a 5% CO_2 incubator at 37 °C. After 8 h, the flow was reversed to an upward orientation at indicated flow rates for the duration of the culture. After 24 h of culture, the medium was replaced with serum-free maintenance medium. Subsequently, media exchanges and sample collections were performed every 48 h for the duration of the culture. Media replacements for the 2D culture coincided with those of the bioreactor. Flow conditions were chosen based on scaling the parameters used in the previous work with this reactor configuration [Powers et al., 2002a], which ensure that shear stress is within a physiological range and the flow rates are sufficient to provide cellular oxygenation.

Live/Dead Staining and Imaging

Cell viability was visualized qualitatively using live/dead cytotoxicity assay kit (Life Technologies, Carlsbad, CA). At specified time points, scaffolds were retrieved from the bioreactor and incubated in serum free maintenance media with 1:1000 Calcein AM, 1:500 Ethidium homodimer-1, and 1:1000 Hoechst (to label cell nuclei) at 37 °C in a CO_2 incubator. After 90 mins, the scaffolds were rinsed with fresh media and images were captured on a fluorescent microscope using FITC, Rhodamine, and DAPI filters. Images were overlapped in FIJI.

Quantification of Albumin Production and Total Protein

Albumin secretion was measured from media collected on days 3, 5, and 7 using a rat albumin ELISA kit (Bethyl Labatories, Inc., Montgomery, TX). Albumin production was normalized to the total protein on days 3 and 7 using a bicinchoinic acid (BCA) protein assay kit (Thermo Scientific, Rockford, IL) to account for differences in cell numbers per condition at each time point. Cells were lysed in RIPA buffer (Upstate Biotechnology, Waltham, MA) with protease inhibitors cocktail (Roche, Indianapolis, IN) for 10 mins over ice. Lysed samples were then centrifuged at 10,000 rpm for 5 mins at 4 °C. The supernatant was stored at −80°C, and the BCA assay was performed on thawed supernatants. Conditions were tested in triplicate and the data was statistically analyzed with ANOVA followed by Tukey's test with alpha = 0.05.

Results

Scaffold Design and Characterization

Scaffolds having different open channel geometries, namely, aligned or staggered ellipses and rectangles having nominal lengths of 900 μm and widths of 600 μm with channel spacings of 300 μm were drawn in a CAD file and exported to STL format. Channel packing densities were a function of channel geometry and channel alignment (staggered or aligned), and were 30, 34, and 43 per scaffold for staggered rectangular, aligned rectangular, and staggered elliptical designs, respectively. A low molecular weight PEGDA (700 Da) was selected to minimize swelling, potentially reducing delamination of the hydrogel from the filter. Further, gels made from PEGDA 700 induce moderate cell adhesion, presumably via adsorption of serum or cell-secreted proteins, even when no bioadhesion ligands are incorporated into the gel. Poly(ethylene oxides) with molecular weights below 1500 g/mol have been shown to adsorb proteins [Bergstrom et al., 1995].

Given the specified SLA parameters, the hydrogel scaffolds were polymerized via a rasterizing process termed "hatching", followed by a single border trace of each channel. As a consequence, each open channel is separated by two laser traces in both the rectangular and elliptical designs. The appearance of a typical scaffold following swelling in culture medium is shown in (Fig. 1) to illustrate the relationship between fabrication parameters and final feature resolution.

As illustrated by the representative scaffolds shown in Figure 1, the actual dimensions of the features differ from the nominal dimensions due to post-fabrication swelling of the crosslinked hydrogel. Actual dimensions of PEGDA scaffold channels bonded to PC membranes after equilibrium swelling measured 850 μm by 350 μm (nominal 900 μm by 600 μm) with a 560 m wide hydrogel wall in between channels for rectangular scaffolds, and 698 μm by 313 μm (nominal 900 μm by 600 μm), with a 460 m wide hydrogel wall in between channels for elliptical open channel designs. For adjacent rectangular channels, where the laser border traces are parallel, the thickness of the hydrogel walls between channels is a little over twice the nominal laser beam width after swelling. For adjacent elliptical channels, the curved geometry of the channels leads to some overlap between the laser border traces, explaining the reduced width of the hydrogel wall for channels with more rounded geometries.

Based on these measurements, the nominal degree of swelling is ~150%, consistent with the results previously observed for SLA-driven polymerization of this macromer solution (Chan et al 2010). The vertical thickness of hydrogels fabricated on glass substrates was estimated to be as 175 ± 20 μm. The width of the hydrogel wall between channels was measured for rectangular channel geometries from three different scaffolds and three different wells per scaffold and varied with photoinitiator (PI) concentration and energy density as follows: 0.5% PI and 138 mJ/cm^2 measured 219 ± 10 μm, 1% PI and 138 mJ/cm^2 measured 242 ± 10 μm, and 0.5% PI and 513 mJ/cm^2 measured 297 ± 8 μm. Thus, hydrogel formulations and SLA energy doses modulate the spacing between open channels.

Filter Bonding and Cell Viability

A number of technical approaches were investigated to achieve robust hydrogel bonding to two filter types (track-etched PC and interwoven PVDF) such that the composite hydrogel scaffold-membrane structure would not delaminate during the chemical and mechanical

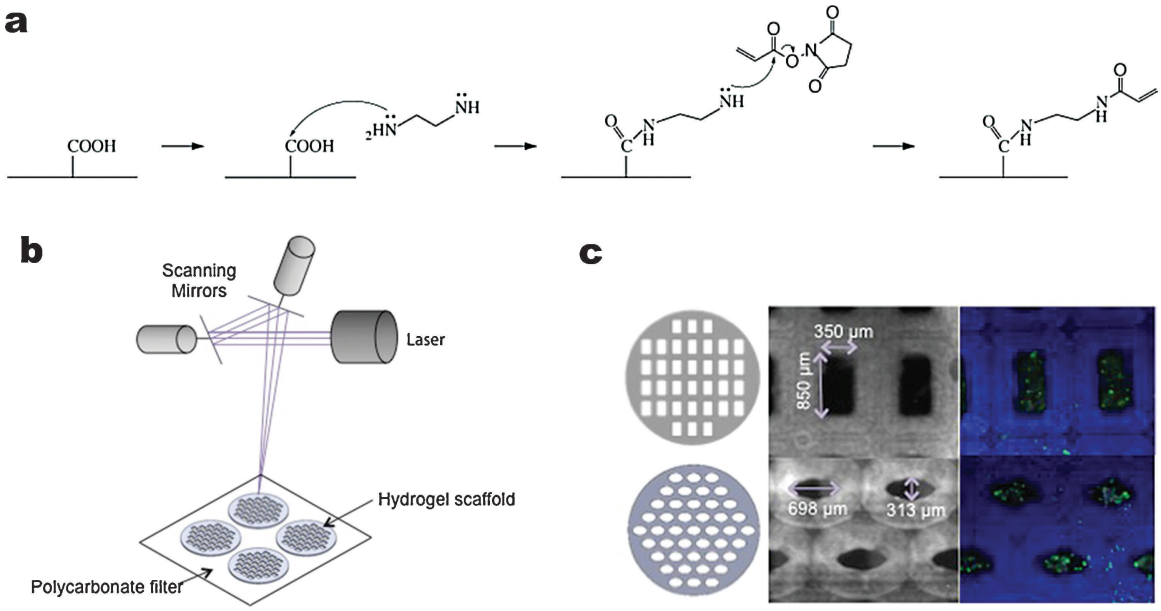

Figure 1. Filter activation and hydrogel scaffold fabrication. PC and PVDF filters were activated by amination and NHS chemistry to expose acrylate groups that participate in free radical polymerization during hydrogel scaffold photopolymerization (a). A stereolithography apparatus (SLA) was used to fabricate PEGDA hydrogel scaffolds on chemically activated PC/PVDF filters. Serial rasterizing of the SLA's ultraviolet laser was used to cure the photosensitive prepolymer resin and form arrays of channels within the hydrogel scaffold. (b). Individual channel borders were outlined by the SLA laser for both rectangular and elliptical channel geometries. As a consequence, open channels were separated by two laser traces for both channel geometries. Aligned rectangular and staggered ellipses had final dimensions on the order of 300 μm in width and 700 to 900 μm in length; both of which promoted hepatocyte viability as shown by a live (green)/dead (red) staining, hydrogel scaffolds retain Hoechst (blue) (c).

stresses of sterilization procedures, crosscontinental shipping, and long-term perfusion flow of up to 1 μL/s, with the additional constraint of ensuring the final composite contained no cytotoxic residues. Parameters and process steps investigated included filter activation chemistry, filter pretreatment with concentrated photoinitiator concentrations, polymerization conditions (laser energy, photoinitiator concentration), and methods of packaging final products for shipment. During filter activation, increasing the plasma treatment time from 15 s to 10 min significantly improved hydrogel binding to PC filters from 2/9 to 14/20 intact scaffolds following the sterilization soak. Increasing the plasma treatment of PC for these times decreases contact angle measurements from 60 to 22 (Kang et. al., 2008), indicating a greater number of –OOH groups exposed on the filter surface for subsequent chemical activation. Scaffolds fabricated on chemically activated PC filters that were shipped taped on glass coverslips and fully hydrated with PBS in coplin jars lead to more intact samples following shipping relative to scaffolds shipped fully hydrated in a 50 mL conical tube.

With the optimal shipping protocol and using a standard 2 h 70% ethanol sterilization protocol (see Methods), we found that pretreating PC membrane filters with photoinitiator, which in theory would mitigate any local interfacial depletion effects due to adsorption of hydrophobic photoinitiator to the membrane, did indeed reduce delamination, from 1/16 (no pretreatment) to 0/16 (with pre-treatment) for scaffolds produced with an optimal energy density (513 mJ/cm^2). More importantly, modulation of the SLA energy dose significantly improved scaffold robustness, as most (9/16) scaffolds delaminated when fabricated with an energy dose of 138 mJ/cm^2, even with 1% photoinitiator present and pretreatment of the filter with photoinitiator. The mechanism of delamination appeared to be insufficient polymerization at the filter interface, suggesting insufficient energy penetration.

We anticipated fewer delamination problems on PDVF filters than on PC filters due to the stark differences in microstructure of the membranes. The track-etch through-holes on the PC membranes result in relatively little surface area for gel-membrane bonding, and also forces a very abrupt interface where stress can be concentrated during swelling. In contrast, the PDVF membranes have a more porous fiber-like architecture that is penetrated by the liquid macromer solution, and after gelation, the gel is physically bonded by virtue of the interpenetrating network around the membrane fibers. Indeed, we saw no delamination of gels formed on PDVF filters post-fabrication. The PC membranes have more desirable optical properties, hence we evaluated both types of membranes in cell culture studies.

Next, the membrane-scaffold constructs were assessed for their robustness to delamination and ability to foster liver cell viability and aggregation under perfusion flow in the bioreactor. The scaffold was designed with open channels to allow facile cell seeding into the channels and then formation of tissue-like structures in the channels under perfusion flow with minimal capture of cells on the upper surface of the scaffold. Calcein AM staining of cells in the scaffold on day 3 demonstrate the localization of cells to the channels with minimum cells located on top of the hydrogel (Fig. 2). Photoinitiator concentration and pretreatment

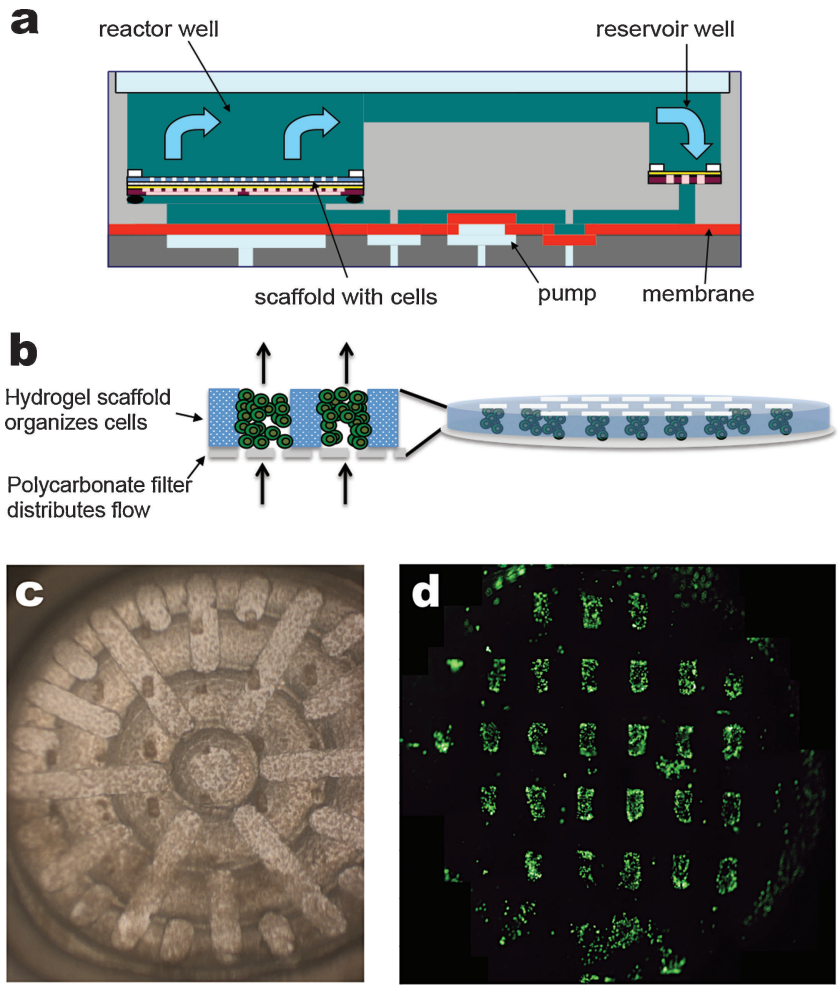

Figure 2. Hydrogel scaffold organizes liver cells in a perfused bioreactor. A perfused bioreactor houses the fabricated hydrogel scaffold and recirculates media through the open channels of the scaffold in direct contact with seeded cells (a). Hydrogel scaffolds organize the cells and tissue formation, while the chemically bound filter distributes flow to the cells in the perfused bioreactor due to its high impedance (b). Tissue formation within the open channels can be observed in situ with phase microscopy on day 3 (c). Calcein AM staining on day 3 demonstrates the majority of cells are localized within the channels exposed to perfusion flow, while minimal cells reside on top of the hydrogel scaffolds where conditions more closely resemble static culture (d).

(for PC membranes) and cell seeding densities were screened to determine conditions that adversely effected cell viability; and images were scored in FIJI to quantify the number of ethidium-stained cell nuclei per channel and the total area of calcein-stained cells per channel for two scaffolds per condition and three images per scaffold. A larger number of dead cells was measured in scaffolds fabricated on PC filters using 1% PI, PI pretreatment, and 138 mJ/cm^2 energy dose relative to the other conditions, and greater area of live cells was measured in scaffolds fabricated with 0.5% PI, no PI pretreatment, and 513 mJ/cm^2 relative to the other conditions (Fig. 3a and c).

Delamination frequency under perfused flow neared 50% for PC scaffolds not pretreated with PI; thus, 0.5% PI, with PI pretreatment, and 513 mJ/cm^2 was used for all subsequent studies. Next, cell seeding densities were screened and similarly scored in FIJI for two scaffolds per condition. Increasing cell seeding density from 75,000 cells per well to 95,000 cells per well decreased the number of ethidium stained cell nuclei per channel and increased the total area of calcein-stained cells per channel after 1 day of perfused culture (Fig. 3d and h).

Formation of Hepatic Spheroids and Maintenance of Liver Specific Functions

Cells seeding densities and flow rates were modulated to determine their effects on tissue morphogenesis in perfused culture within hydrogel scaffolds fabricated on PC filters. Here, higher cell seeding densities were used than those in the viability experiments described above, as the goal was to assess formation of tissue structure and not to discriminate how initial conditions influenced survival. Images of cells maintained in the open channels illustrate the evolution of tissue morphology during perfused culture (Fig. 4). Cells initially condense into larger structures on day 3, and by day 7 smaller cell aggregates are observed. Cell viability was maintained throughout the culture for both cell seeding densities and flow rates.

Notably, scaffolds remained intact for this prolonged perfused culture.

Subsequently, the maintenance of liver specific function was examined with hydrogel scaffolds fabricated on each filter type (PC or PVDF) under 0.3 or 1 μL/s flow rates relative to 2D controls. The total protein measured indicates the retention of cells during culture and loss of cells was only observed in the low flow PVDF and 2D control conditions (Fig. 5a). Albumin secretion did not vary between the perfused culture conditions. Albumin production declined for perfused and static cultures. Importantly, the rate of decline was lower within the scaffolds for each flow rate and filter type relative to 2D cultures (Fig. 5b). Furthermore, tissue formation at day 7 appeared similar within hydrogel scaffolds fabricated on PC and PVDF filters (Fig. 5c and d).

Improvements in albumin production were assessed in 2D and bioreactor cultures with scaffolds fabricated on PVDF filters cultured with and without EGF added to the culture medium. EGF supplementation did not change the retention of cells in the bioreactor culture at the day 7 time point (Fig. 6a), however, significant improvements in albumin production were observed in the bioreactor at the day 3 time point and in the 2D cultures at day 7 (Fig. 6b). Notably, bioreactor cultures with EGF supplementation maintained levels of albumin production while this liver specific function declined in 2D cultures despite the addition of EGF to the medium.

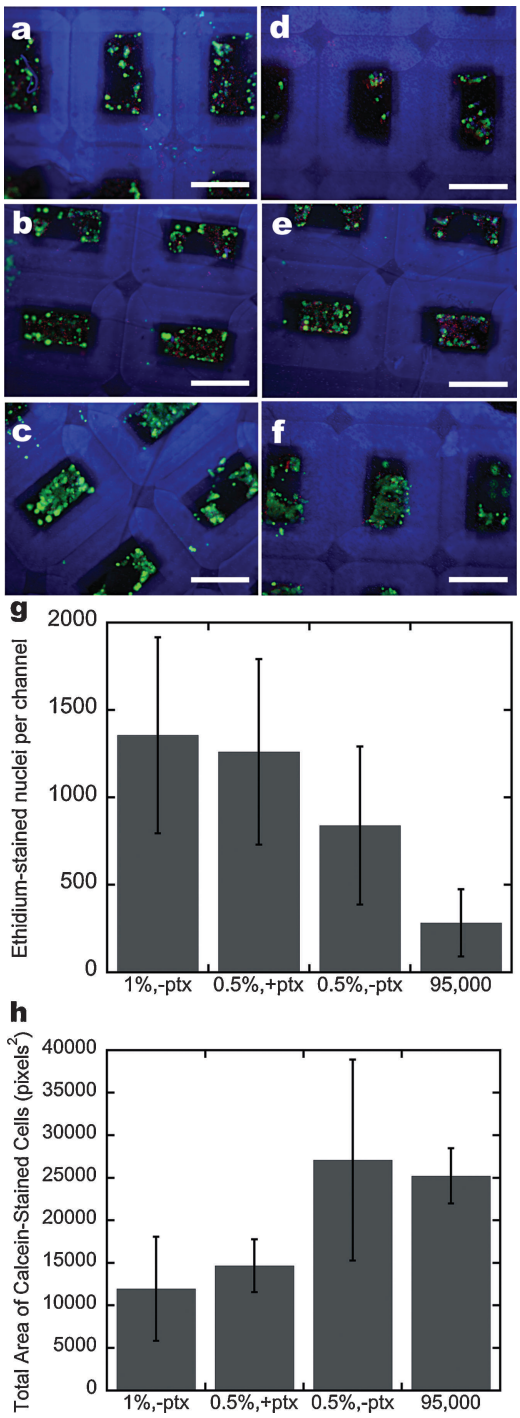

Figure 3. Continued.

Discussion

Improvements of in vitro culture systems for prolonging the maintenance of liver specific functions of hepatocytes aim to recapitulate their complex physiological microenvironment. Microfluidic platforms provide nutrient exchange, introduce shear stresses, and enable the development of physiological oxygen concentration gradients. Scaffolds within microfluidic platforms provide structural support and introduce biochemical and mechanical cues to direct tissue formation (Fig. 2). While past scaffold designs include rigid materials to withstand perfused flow, these mechanical properties are not ideal for the culture of hepatocytes. In 2D culture formats, several reports have indicated hepatocytes adopt a dedifferentiated phenotype when cultured on stiff matrices, while they maintain their differentiated state on soft matrices [Fassett et al., 2006; Hansen et al., 2005; Mehta et al., 2010; Semler et al., 2000b]. While the microenvironment of the

Figure 3. Liver cell viability in perfused scaffolds is a function of scaffold crosslinking conditions and initial seeding density. Effects of crosslinking conditions (a-c) were tested by seeding cells at a density of 75,000 cells/well (2,200 cells/channel) and maintaining cultures under μL/s/scaffold flow rate (0.03 μL/s/channel) for 24 h where flow was reversed after the initial 8 h of culture then in situ staining with calcein AM, ethidium homodimer-1, and Hoechst after 1 day of culture. The range of polymerization conditions tested were: photoinitiator pretreatment and 1% photoinitiator concentration in the prepolymer fabricated with 138 mJ/cm2 energy dose (a), photoinitiator pretreatment and 0.5% photoinitiator concentraton in the prepolymer fabricated with 513 mJ/cm2 energy dose (b), and no photoinitiator pretreatment and 0.5% photoinitiator concentration in the prepolymer fabricated with 513 mJ/cm2 (c). Viability of cells seeded at a range of cell seeding densities was tested after 1 day of perfused culture at 1 μL/s flow rate within scaffolds fabricated with photoinitiator pretreatment, 0.5% photoinitiator concentration, and 513 mJ/cm2 energy dose (d-f): 25,000 (740) (d), 75,000 (2,200) (e), or 95,000 cells/well (2,800 cells/channel) (f). Live cells are stained in green with Calcein AM, dead cells are stained in red with ethidium homodimer-1, cell nuclei and hydrogel scaffolds (nonspecifically stained) were stained with Hoechst, and white scale bars represent 500 μm. Quantification of the number of ethidium-stained nuclei (g) and the area of calcein-stained cells per channel (h) scored in ImageJ for two scaffolds per condition and three images per scaffold. In the quantification the conditions: 1% photoinitiator no pretreatment, 0.5% photoinitiator with pretreatment, and 0.5% photoinitiator no pretreatment where tested with a cell seeding density of 75,000 cells/well and 0.5% photoinitiator with pretreatment was tested using the cell seeding density of 95,000.

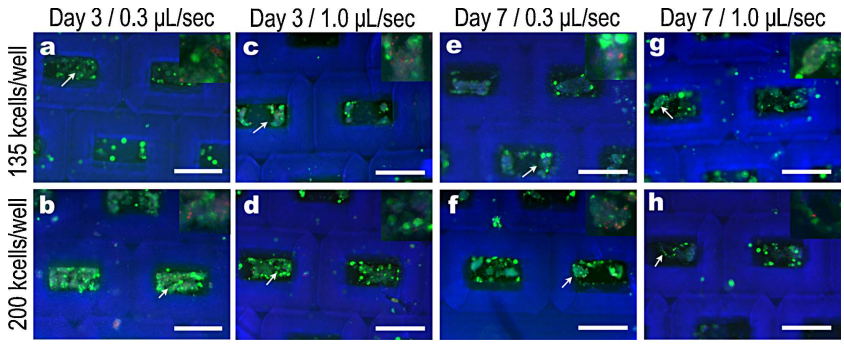

Figure 4. Maintenance of cell viability cultured within hydrogel scaffolds perfused at multiple flow rates and cell seeding densities. Cell viability was assessed for two different cell seeding densities: 135,000 (4,500) (a, c, e, g) and 200,000 cells/well (6,700 cells/channel) (b, d, f, h) at day 3 (a-d) and day 7 (e-h) and 0.3 (a, b, e, f) and 1 µL/s (c, d, g, h) within scaffolds fabricated on PC filters. Live cells are stained in green with calcein AM, dead cells are stained in red with ethidium homodimer-1, cell nuclei and hydrogel scaffolds (nonspecifically stained) were stained with Hoechst, and white scale bars represent 500 µm. White arrows indicate the region that is magnified the inset.

3D scaffold environment fosters formation of 3D cultures with enhanced functions compared to 2D cultures [Powers et al., 2002a] and 2002b), cells immediately adjacent to the scaffold still experience a stiff environment even though they are "3D". In separate ongoing studies with human liver cells cultured in hydrogel compared stiff plastic scaffold, the hydrogel scaffold is associated with lower basal production of inflammatory cytokines compared to the stiff scaffold (Griffith, Wells et al, unpublished data). Additionally, hydrogel scaffolds are permeable to oxygen, nutrients, and most cell-secreted autocrine factors, but whether this offers an advantage to tissue performance is currently unexplored. Thus, we have photopatterned compliant and biocompatible hydrogel-based scaffolds bonded to multiple filter types using SLA that are capable of withstanding perfused flow. These scaffolds support the culture of post-seeded cells while employing bonding chemistries that promote cell viability and enable the maintenance of liver specific functions (Figs. 1 and 2).

Fabricating patterned hydrogels chemically bonded to polymer substrates remains challenging due to hydrogel swelling and difficulty of coupling chemistries. In this report, we demonstrate bonding of a hydrogel scaffold to a polymer-based filter by employing a coupling chemistry that is non-toxic to cells, yet robust enough to withstand shipping and multi-day perfused flow as a structural support for post-seeded liver cells in a bioreactor. Despite the selection of low M_w PEG-diacrylate (700 Da) to limit swelling and reduce potential of delamination from the filter, hydrogel delamination was a major technical challenge that was overcome by optimizing the filter chemical activation, filter pretreatment with photoinitiator (to saturate the filter and ensure concentrated local generation of free radicals) and polymerization conditions (photoinitiator concentration and energy dose). Formulas that maximized hydrogel bonding to the filter were tested to determine which conditions maintained cell viability. Increasing prepolymer photoinitiator concentration led to lower delamination frequencies, but reduced cell viability (Fig. 3). Alternatively, increasing the SLA energy dose, while employing a moderate photoinitiator concentration and increasing the cell seeding density maintained cell viability while reducing delamination rates for prolonged perfused cultures employing a high and low flow rate lasting 1 week (Fig. 4).

Albumin production, an indicator of hepatocellular metabolic function, was measured to assess whether residual components from the filter activation adversely affected hepatocyte behavior, using standard 2D cultures as a control. As expected based on many prior studies in the literature [Ebrahimkhani et al., 2014; LeCluyse et al., 2012; Powers et al., 2002a; Powers et al., 2002b], albumin production in 2D cultures declined precipitously from the first post-isolation measurement (day 3) to day 7 in the absence of EGF (Figs. Fig. 5b, Fig. 6b) with the decline mitigated by the pr
esence of 10 ng/mLEGF (Fig 6b); differences in the absolute magnitude of the first post-isolation time point in these figures are within the range of those observed for primary cell isolates in the first isolation time point. In the absence of EGFAlbumin production was higher in 2D cultures at the early time point relative to cultures employing both PC and PVDF filters perfused with two flow rates (0.3 and 1 µL/s). One possible cause for this initial difference is that 2D cultures may facilitate accumulation of autocrine factors due to higher cell seeding concentrations and diffusion-based transport (150K cells in 0.5 mL for 2D cultures and 200 K cells in 1.3 mL for 2D culture and bioreactor, respectively); whereas, in the perfusion system, autocrine ligands are actively transported and unable to be recaptured by cell surface receptors (Fig. 5). EGF, an autocrine epidermal growth factor receptor (EGFR) ligand produced by liver cells, is commonly added to hepatocyte cultures to regulate survival and many hepatocyte functions through EGFR activation. In 3D cultures, EGF has been shown to promote tissue formation and greater formation of ECM [Abu-Absi et al., 2002]; [Michalopoulos et al., 2001]. In microwell geometries that facilitated the accumulation of autocrine factors, albumin production of 3D static hepatocyte cultures did not improve upon addition of EGF, but was significantly diminished when EGFR was blocked [Williams et al., 2011]. In our unpublished data employing polycarbonate scaffolds in perfused 3D cultures, the addition of EGF to 3D perfused cultures was necessary for the extensive formation of canalicular networks and retention of canalicular bile acid retention

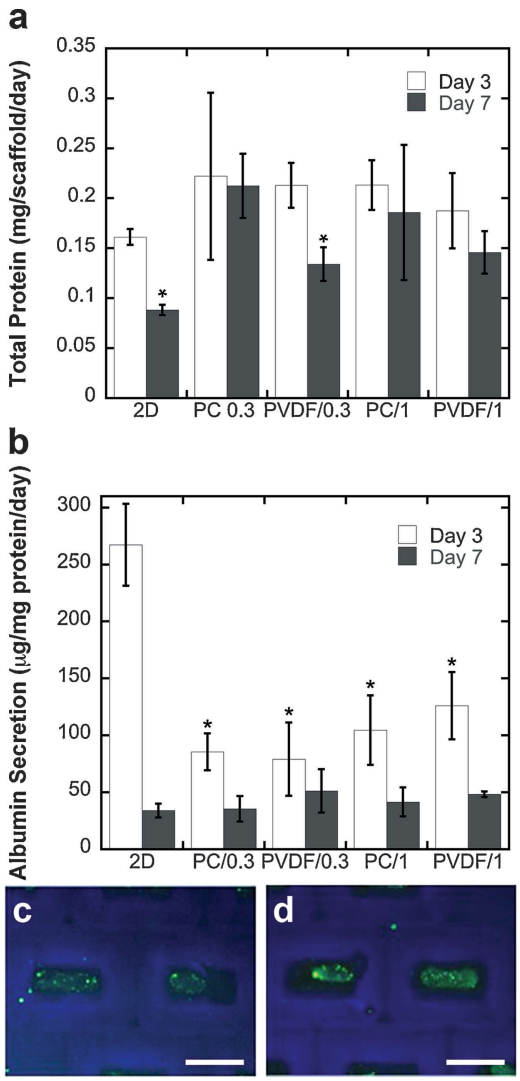

Figure 5. Hydrogel scaffolds promote cell retention and prolong the maintenance of hepatocyte metabolic functions. A BCA assay performed on scaffolds seeded with 200,000 cells/well (6,700 cells/channel) and 2D cultures seeded with 150,000 cells/well (75,000 cells/cm2) at days 3 and 7 indicates the retention of total protein within each type of scaffold at 0.3 μL/s and 1 μL/s flow rates (a). The amount of albumin secreted per scaffold over the course of the study was measured from the collected media (b). Similar tissue formation occurred by within the open channels of scaffolds fabricated on PVDF (c) and PC (d) filters by day 7 when cultured with a 1 μL/s flow rate. Live cells are stained in green with calcein AM, dead cells are stained in red with ethidium homodimer-1, cell nuclei and hydrogel scaffolds (nonspecifically stained) were stained with Hoechst, and white scale bars represent 500 μm. Significant differences in total protein on Day 7 relative to Day 3 are denoted by *. Significant differences in albumin production at each time point relative to 2D are denoted by * based on ANOVA with $p<0.05$, $n>2$.

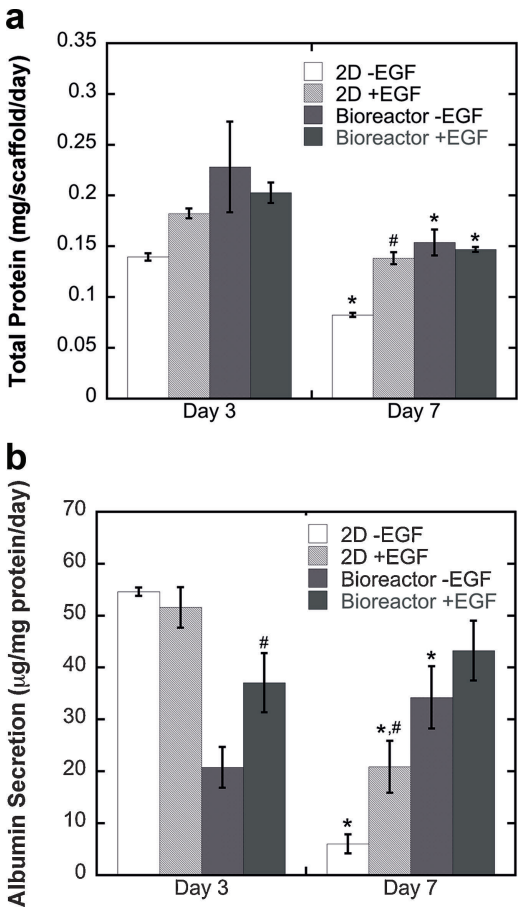

Figure 6. Addition of EGF to hepatocyte culture medium improves albumin production in both static and perfused hepatocyte cultures. Hydrogel scaffolds fabricated on PVDF filters and perfused at 0.3 μL/s flow rate were seeded with 200,000 cells/well (6,700 cells/channel), and 2D cultures were seeded with 150,000 cells/well (75,000 cells/cm2) on collagen coated tissue culture polystyrene. A BCA performed on the cultures at each time point indicate the retention of total protein for each culture condition (a). The amount of albumin secreted over the course of the study was measured from the collected media (b). Significant differences at each time point relative to the respective culture configuration with no EGF are denoted by # with $p<0.05$, $n>3$. Significant differences between time points per condition is based on Tukey's test are denoted by * with $p<0.05$, $n>3$. Fabrication of hydrogel scaffolds for perfused culture offers greater physiologically relevant microenvironments for liver cells to potentially improve drug toxicity testing. Here, hydrogel scaffolds were chemically coupled to commercially available filters that were chemically activated by photopatterning with stereolithography (a). In a perfused bioreactor, the hydrogel scaffold is designed with open channels to organize cells and tissue formation in contact with fluid flow to facilitate mass transport of oxygen, nutrients, and waste, while the filter homogeneously distributes fluid flow (b).

mimicking the microarchitecture of the liver. In this study, the addition of EGF did not improve the retention of cells, but significantly improved albumin production in the bioreactor (Fig. 6). In fact, long-term albumin production rates were significantly higher in the bioreactor relative to the 2D cultures. The production rates in this system translate to ~35 to 42 pg/cell/day, which falls within the range of albumin secretion rates reported for a variety of reactor configurations ranging from 2 to upwards of 150 pg/cell/day [Tsang et al., 2007; Ong et al., 2008; Powers et al., 2002b]. Thus, the filter activation chemistry employed herein is non-toxic and does not alter the metabolic functions of primary hepatocytes cultured under perfused flow.

There lies opportunity to further optimize hepatocyte culture through modification of culturing procedures and the bioactive design of the hydrogel material. In this study, individual cells in suspension were seeded in the bioreactor. Powers et al. reported that the aggregation of hepatocytes prior to seeding increased albumin production rates two-fold relative to seeding single cells in a

bioreactor, while single cell aggregates experience a drop in the rate of albumin production after 4 days of perfused culture that corresponded to a loss in tissue-like structure (2002a). Additionally, faster kinetics of spheroidal formation is associated with fewer dead cells and improved spheroid morphology [Brophy et al., 2009]; thus, modifying the culturing procedures of the report herein by seeding aggregated hepatocytes rather than individual cells in suspension may further improve albumin production rates. Another approach to improve the culture lies in increasing material adhesivity to better retain cell numbers during perfused culture yet enabling cell-cell interactions for spheroidal formation. Freshly isolated rat hepatocytes have been shown to express α_1, α_5, and β_1 and syndecans -1, -2, and -4 on the cell surface with integrin expression shifts away from α_5 subunits and towards $\alpha_6\beta_1$ during in vitro culture [Tsang et al., 2007; Weiner et al., 1996]. A number of cell adhesive peptides that engage these integrins and syndecans have been reported, and can be explored to capture the dynamic integrin expression of hepatocytes [Araki et al., 2009; Kikkawa et al., 2011; Tsang et al., 2007]. Incorporation of cell adhesive peptides into scaffolds fabricated with SLA is readily achieved and has been report through conjugation with RGD and polymerization with acrylated collagen [Chan et al., 2010; Chan et al., 2012]. Ideally, cell adhesion would be localized to the interior walls of the open channels to eliminate cell adhesion on the top of the scaffold where they would be isolated from the perfusion flow.

Here, we developed an approach to covalently couple photo-patterned hydrogels having open channels to commercially activated filters using SLA for post-seeding cells within a perfused bioreactor. We have scaled up the polymerization procedure with the SLA in order to test filter activation, photoinitiator pretreatment, and polymerization conditions were optimized to prevent delamination during shipping, sterilization, and culture while promoting cell viability and maintenance of liver specific functions. After 7 days of perfused culture, hydrogel scaffolds remained intact and primary hepatocytes exhibited higher levels of albumin production relative to 2D controls demonstrating the biocompatibility of the hydrogel bonding chemistry. Due to the versatility of the PEG-acrylate polymer chemistry, this system can be tailored to suit a number of bioreactor applications outside of liver tissue engineering by incorporating various biofunctional ligands with SLA-polymerizable hydrogels and patterning them in a variety of spatially patterned channel geometries. In addition to their high material tuneability, hydrogel scaffolds have mechanical and transport properties more similar to native tissue and could thus improve numerous bioreactor applications for perfused in vitro culture of a number of highly metabolically active cell types. This approach can be implemented in a number of bioreactor applications requiring soft materials capable of withstanding perfused flow, providing a platform for preserving engineered tissue-specific function in vitro. Further, the robust coupling of the hydrogel scaffold to the filter as demonstrated by the ability to ship them transcontinentally, sterilize them with multiple procedures, and culture under perfused flow makes this approach commercially viable, useful for high-throughput drug testing applications.

The authors thank Emma Gargus for the provision of chemically activated filters. Financial support for this research was provided by NIH NCATS (5UH2TR000496-02), the National Science Foundation (NSF STC Emergent Behavior of Integrated Cellular Systems), the Defense Advanced Projects Agency BAA-11-73 Microphysiological Systems: W911NF-12-2-0039 Barrier-Immune-Organ: Microphysiology, Microenvironment Engineered Tissue Construct Systems (BIO-MIMETICS), NSF Grant 0965918 IGERT at UIUC: Training the Next Generation of Researchers in Cellular and Molecular Mechanics and Bionanotechnology, NSF Graduate Research Fellowship Grant DGE-1144245, and Center for Environmental Health Sciences P30-ES002109. The authors declare no conflict of interest.

References

Abu-Absi SF, Friend JR, Hansen LK, Hu W-S. 2002. Structural polarity and functional bile canaliculi in rat hepatocyte spheroids. Exp Cell Res 274:56–67.

Ananthanarayanan A, Narmada BC, Mo X, McMillian M, Yu H. 2011. Purpose-driven biomaterials research in liver-tissue engineering. Trends Biotechnol 29(3): 110–118.

Araki E, Momota Y, Tanioka M, Hozumi K, Nomizu M, Miyachi Y, Utani A. 2009. Clustering of syndecan-4 and integrin beta1 by laminin alpha3 chain–derived peptide promotes keratinocyte migration. Mol Biol Cell 20:3012–3024.

Arcaute K, Mann BK, Wicker RB. 2006. Stereolithography of three-dimensional bioactive poly(ethylene glycol) constructs with encapsulated cells. Ann Biomed Eng 34:1429–1441.

Bajaj P, Marchwiany D, Duarte C, Bashir R. 2013. Patterned three-dimensional encapsulation of embryonic stem cells using dielectrophoresis and stereolithography. Advanced Healthcare Mater 2:450–458.DOI: 10.1002/adhm.201200318.

Bergstrom K, Osterberg E, Holmberg K, Hoffmann AS, Schuman TP, Kozlowski A, Harris JM. 1995. Effects of branching and molecular weight of surface-bound poly(ethylene oxide) on protein rejection. J Biomater Sci. Polym Ed 6: 123–132.

Brophy CM, Luebke-Wheeler JL, Amiot BP, Khan H, Remmel RP, Rinaldo P, Nyberg SL. 2009. Rat hepatocyte spheroids formed by rocked technique maintain differentiated hepatocyte gene expression and function. Hepatology 49:578–586.

Chan V, Jeong JH, Bajaj P, Collens M, Saif T, Kong H, Bashir R. 2012. Multi-material bio-fabrication of hydrogel cantilevers and actuators with stereolithography. Lab Chip 12:88–98.

Chan V, Zorlutuna P, Jeong JH, Kong H, Bashir R. 2010. Three-dimensional photopatterning of hydrogels using stereolithography for long-term cell encapsulation. Lab Chip 10:2062–2070.

Coger R, Toner M, Moghe P, Ezzell RM, Yarmush ML. 1997. Hepatocyte aggregation and reorganization of EHS matrix gel. Tissue Eng 3:375–390.

Dash A, Inman W, Hoffmaster K, Sevidal S, Kelly J, Obach RS,…, Tannenbaum SR. 2009. Liver tissue engineering in the evaluation of drug safety. Expert Opin Drug Metab Toxicol 5:1159–1174.

Dhariwala B, Hunt E, Boland T. 2004. Rapid prototyping of tissue-engineering constructs, using photopolymerizable hydrogels and stereolithography. Tissue Eng 10:1316–1322.

Domansky K, Inman W, Serdy J, Dash A, Lim MHM, Griffith LG. 2010. Perfused multiwell plate for 3D liver tissue engineering. Lab Chip 10:51–58.

Ebrahimkhani MR, Shepard Neiman JA, Raredon MSB, Hughes DJ, Griffith LG. 2014. Bioreactor technologies to support liver function in vitro. Adv Drug Delivery Rev 69-70:132–157.

Fassett J, Tobolt D, Hansen LK. 2006. Type I collagen structure regulates cell morphology and EGF signaling in primary rat hepatocytes through cAMP-dependent protein kinase A. Mol Biol Cell 17:345–356.

Godoy P, Hewitt NJ, Albrecht U, Andersen ME, Ansari N, Bhattacharya S,…, Hengstler JG. 2013. Recent advances in 2D and 3D in vitro systems using primary hepatocytes, alternative hepatocyte sources and non-parenchymal liver cells and their use in investigating mechanisms of hepatotoxicity, cell signaling and ADME. Arch Toxicol 87:1315–1530.

Griffith LG, Wells A, Stolz DB. 2014. Engineering Liver. Hepatology (Baltimore, Md.) DOI: 10.1002/hep.27150.

Hansen LK, Mooney DJ, Vacanti JP, Ingber DE. 1994. Integrin binding and cell spreading on extracellular matrix act at different points in the cell cycle to promote hepatocyte growth. Mol Biol Cell 5:967–975.

Hansen LK, Wilhelm J, Fassett JT. 2005. Regulation of hepatocyte cell cycle progression and differentiation by type I collagen structure. Curr Top Dev Biol 72:205–236.

Kang SM, Yoon SG, Yoon DH. 2008. Surface treatment of polycarbonate and polyethersulphone for SiNx thin film deposition. Thin Solid Films 516:1405–1409.
Khetan S, Burdick JA. 2011. Patterning hydrogels in three dimensions towards controlling cellular interactions. Soft Matter 7:830–838.
Kikkawa Y, Kataoka A, Matsuda Y, Takahashi N, Miwa T, Katagiri F, Nomizu M. 2011. Maintenance of hepatic differentiation by hepatocyte attachment peptides derived from laminin chains. J Biomed Mater Res. Part A 99:203–210.
LeCluyse EL, Witek RP, Andersen ME, Powers MJ. 2012. Organotypic liver culture models: meeting current challenges in toxicity testing. Crit Rev Toxicol 42:501–548.
Lutolf MP, Hubbell JA. 2005. Synthetic biomaterials as instructive extracellular microenvironments for morphogenesis in tissue engineering. Nat Biotechnol 23:47–55.
Mehta G, Williams CM, Alvarez L, Lesniewski M, Kamm RD, Griffith LG. 2010. Synergistic effects of tethered growth factors and adhesion ligands on DNA synthesis and function of primary hepatocytes cultured on soft synthetic hydrogels. Biomaterials 31:4657–4671.
Melchels FPW, Feijen J, Grijpma DW. 2010. A review on stereolithography and its applications in biomedical engineering. Biomaterials 31:6121–6130.
Michalopoulos GK, Bowen WC, Mulè K, Stolz DB. 2001. Histological organization in hepatocyte organoid cultures. Am J Pathol 159:1877–1887.
Moghe P, Berthiaume V, Ezzell F, Toner RM, Tompkins M, Yarmush RG. 1996. Culture matrix configuration and composition in the maintenance of hepatocyte polarity and function. Biomaterials 17:373–385.
Ong S-M, Zhang C, Toh Y-C, Kim SH, Foo HL, Tan CH,…, Yu H. 2008. A gel-free 3D microfluidic cell culture system. Biomaterials 29:3237–3244.
Powers MJ, Domansky K, Kaazempur-mofrad MR, Kalezi A, Capitano A, Upadhyaya A. 2002. Grif, L. G.. A microfabricated array bioreactor for perfused 3D liver culture. Biotechnol Bioeng 78:257–269.
Powers MJ, Janigian DM, Wack KE, Baker CS, Stolz DB, Griffith LG. 2002b. Functional behavior of primary rat liver cells in a three-dimensional perfused microarry bioreactor. Tissue Eng 8:499–513.
Powers MJ, Rodriguez RE, Griffith LG. 1997. Cell-substratum adhesion strength as a determinant of hepatocyte aggregate morphology. Biotechnol Bioeng 53:415–426.
Semler EJ, Lancin P, a Dasgupta, Moghe PV. 2005. Engineering hepatocellular morphogenesis and function via ligand-presenting hydrogels with graded mechanical compliance. Biotechnol Bioeng 89:296–307.
Semler EJ, Ranucci CS, Moghe PV. 2000a. Mechanochemical manipulation of hepatocyte aggregation can selectively induce or repress liver-specific function. Biotechnol Bioeng 69:359–369.
Semler EJ, Ranucci CS, Moghe PV. 2000b. Mechanochemical manipulation of hepatocyte aggregation can selectively induce or repress liver-specific function. Biotechnol Bioeng 69:359–369.
Tsang VL, Chen AA, Cho LM, Jadin KD, Sah RL, DeLong S,…, Bhatia SN. 2007. Fabrication of 3D hepatic tissues by additive photopatterning of cellular hydrogels. FASEB J 21:790–801.
Underhill GH, Chen A, a Albrecht, Bhatia SN. 2007. Assessment of hepatocellular function within PEG hydrogels. Biomaterials 28:256–270.
Weiner OH, Zoremba M, Gressner a. 1996. Gene expression of syndecans and betaglycan in isolated rat liver cells. Cell Tissue Res 285:11–16.
Williams CM, Mehta G, Peyton SR, Zeiger AS, Vliet, Van KJ, Griffith, LG. 2011. Autocrine-controlled formation and function of tissue-like aggregates by primary hepatocytes in micropatterned hydrogel arrays. Tissue Eng. Part A 17:1055–1068.
Zorlutuna P, Jeong JH, Kong H, Bashir R. 2011. Stereolithography-based hydrogel microenvironments to examine cellular interactions. Adv Funct Mater 21:3642–3651.